Check for updates

Comprehensive analysis of novel cubic HgCrO₃ perovskite: a first principles, structural, thermodynamic, and magnetic properties study for spintronic applications

Junaid Khan,[ab] Murefah mana Al-Anazy,[c] El Sayed Yousef,[de] Datta D,[f] Ramesh Sharma [ID] *[f] and A. J. A. Moayad*[g]

The main goal of modern manufacturing is to create products that are affordable, eco-friendly, and energy-efficient. With a focus on HgCrO₃, this study sought to discover molecules that meet these requirements. The structural, electrical, thermodynamic, and transport properties of the material were investigated using Wien2K, a full-potential, linearized augmented plane wave program (FP LAPW). Utilizing the generalised gradient approximation (GGA) and lattice constants that have previously produced excellent theoretical and practical findings, structural optimization was carried out. Calculated HgCrO₃ magnetic characteristics show that the Cr and Hg atoms are the main contributors to magnetism. Over a temperature range of 0–1200 K and a pressure range of 0–196 GPa, thermodynamic characteristics were evaluated. The thermoelectric properties of HgCrO₃ were evaluated using the Boltzmann transport method provided by the BoltzTrap program. This analysis revealed that at room temperature, the figures of merit (*ZT*) values for HgCrO₃ were nearly equal to one. A *ZT* value close to one indicates that a material has excellent thermoelectric properties and can efficiently convert heat into electricity or *vice versa*. This investigation highlights the promising thermoelectric capabilities of HgCrO₃, which could contribute to more sustainable and energy-efficient technologies in the future.

1. Introduction

Perovskite oxides, an inorganic substance, have attracted a lot of attention lately due to their exceptional abilities in the areas of electrical, structural, optical, thermoelectric, and elastic behaviours. These materials have a variety of crystalline phases and physicochemical characteristics, including ferroelectricity, ferro-elasticity, anti-ferroelectricity, and others.[1–4] In the subject of spintronics, which studies ways to harness electron spin to store, process, and transfer information, ferromagnetic perovskite materials in particular have grown in importance. The flexible crystal structure of perovskite oxides is a key

characteristic that allows for the development of materials with diverse electrical and other properties. To maintain the stability of the ABO₃ compound structure in perovskites, a standard cubic ABO₃ crystal structure is commonly employed. In this structure, 'A' and 'B' represent two different cations, 'O' stands for an anion, and the radius of 'B' is typically smaller than that of the 'A-cation. In an ideal cubic ABO₃ structure, an oxygen atom typically occupies the unit cell's centre. This arrangement also places a 'B' atom at the centre, with another atom often located at one of the cell's corners. This structural flexibility is crucial for the versatile properties of perovskite oxides, making them highly attractive for various applications, including in the field of materials science, where tailored properties are essential for technological advancements. The ability to fine-tune perovskite structures allows for the creation of materials with specific electrical, magnetic, and optical properties, contributing to innovations in electronic devices, solar cells, and more.[5–9] Recent research has been focused on perovskite materials composed of rare earth (RE) and transition metal (TM) atoms, known as RE-TM-O₃ perovskites. Substituting some cations (B) or TM elements with magnetic counterparts has led to unexpected magneto-electric and multiferroic properties in these materials.[8,10] These properties have garnered significant attention due to their potential applications in data storage,

[a] Department of Physics Khushal Khan Khattak University, Karak, Pakistan

[b] Department of Physics Kohat University of Science and Technology, Kohat, Pakistan

[c] Department of Chemistry, College of Sciences, Princess Nourah bint Abdulrahman University (PNU), P.O. Box 84428, Riyadh, 11671, Saudi Arabia

[d] Research Center for Advanced Materials Science (RCAMS), King Khalid University, Abha 61413, P. O. Box, 9004, Saudi Arabia

[e] Physics Dep., Faculty of Science, King Khalid University, P. O. Box 9004, Abha, Saudi Arabia

[f] Dept. of Applied Science, Feroze Gandhi Institute of Engineering and Technology, Raebareli 229001, Uttar Pradesh, India. E-mail: sharmadft@gmail.com

[g] Department of Materials Science, Malawi University of Science and Technology, P. O. Box, 5196, Limbe, Malawi. E-mail: mailme_moya123@rediffmail.com

spintronics, and next-generation electronic devices. These perovskite substances exhibit both ferromagnetic and ferro-electric ordering, which are interconnected through strain or spin interactions. This unique combination of properties makes them promising candidates for various technological advancements. Researchers have utilized *ab initio* techniques to study the magnetic and electrical characteristics of different perovskites, furthering our understanding of their potential in emerging technologies. As a result, the exploration of RE-TM-O$_3$ perovskites has opened up exciting possibilities for innovative materials with multifunctional properties that could revolutionize electronic and magnetic devices.[11–13] For instance, M. Yaseen *et al.* in 2020 came to the conclusion that the PRCrO$_3$ compound's viability for spintronics applications was proven based on its electrical and magnetic properties.[14] Rashid *et al.* conducted a study using density functional theory (DFT) with the mBJ approximation to investigate the electronic and magnetic properties of the cubic CeCrO$_3$ compound in the ferromagnetic (FM) phase.[15] Their research revealed that CeCrO$_3$ exhibits a total magnetic moment of 4.0 μ_B and possesses half-metallic and ferromagnetic properties. In addition to CeCrO$_3$, recent studies have focused on other compounds like CaCrO$_3$, BaCrO$_3$, and SRCrO$_3$, with a particular emphasis on the length of the Cr–O bond.[11] Materials based on RCrO$_3$ compounds demonstrate remarkable adaptability and exceptional physical properties. These materials exhibit characteristics such as the magnetocaloric effect (MCE), exchange bias, and magnetization reversal, making them attractive for various applications. Despite the growing interest in transition metal oxides and their potential applications, there is currently a gap in the literature regarding the physical properties of RCrO$_3$ compounds (where X = Ca, Sr, Ba, Hg, *etc.*) for use in electrical or spintronic devices.[16,17] Understanding the physical properties of these materials is crucial for designing and implementing high-performance devices. Researchers also explore non-equilibrium growth conditions, such as molecular beam epitaxy (MBE) and other physical vapor deposition techniques, to create stable phases of novel materials with tailored properties.

This study aims to explore the structural, thermoelectric, and magnetic properties of HgCrO$_3$, a cubic perovskite material, to assess its potential industrial applications. To achieve this, the study utilizes the FP-LAPW-GGA (PBE) approach, a computational method commonly used for electronic structure calculations. One noteworthy aspect of this research is that it appears to be the first of its kind to investigate these specific properties of HgCrO$_3$. The lack of existing information on this material highlights the novelty of the study. This pioneering effort to delve into the material's characteristics could potentially serve as a catalyst for further research in this area. Understanding the structural, thermoelectric, and magnetic properties of HgCrO$_3$ is essential for unlocking its industrial potential and expanding its application in various fields. This study represents a crucial step toward harnessing the unique properties of HgCrO$_3$ for technological advancements and innovations.

2. Computational approach

The study focused on evaluating various properties of HgCrO$_3$, including its structural, magnetic, elastic, and electronic characteristics. To conduct this assessment, to employed the Density Functional Theory (DFT)[18,19] framework and utilized the FP-LAPW tool[20] from WIEN2k,[21] which is a widely used computational method for electronic structure calculations. One notable aspect of their study is that they incorporated the spin–orbit effect using semi-relativistic techniques, which is essential for accurately modelling the electronic behaviour of materials with heavy elements like mercury (Hg). Understanding these properties is crucial for gaining insights into the behaviour and potential applications of HgCrO$_3$. The combination of advanced computational tools and the consideration of the spin–orbit effect allows for a comprehensive analysis of this material. Such studies contribute to our understanding of materials with unique characteristics and can inspire further research in areas where HgCrO$_3$ may find practical applications. DFT calculations were used to determine the magnetoelectronic characteristics while taking exchange and correlations into consideration. The structural optimization has been performed employing generalized gradient approximation method (PBE-GGA). For this, the charge convergence requirement of 10–5 has been established as their convergence condition, and the plane wave cut off has been set at 450 eV with a k-grid of $10 \times 10 \times 10$. The convergence criterion for the interaction forces between atoms is set to 0.01 eV Å^{-1}. We employed a plane wave cut-off value of $R_{MT} \times K_{max} = 7$ to obtain convergence in the basis set and discovered the MT radius to be 1.63, 1.54, 1.48 Bohr for Hg, Cr, and O. We increased the radial eigenfunctions of the muffin-tin spheres by spherical harmonics up to $l_{max} = 10$ in order to enhance wave functions within the spheres.[22,23] Additionally, we increased the interstitial region's potential Fourier charge density up to $G_{max} = 14$. Furthermore, the study extended its focus to explore thermoelectric transport properties, utilizing the quasi-harmonic Debye model and the Boltz-TraP algorithm.[24,25] Due to the fact that it mostly depend on the denser *k*-points, the k-mesh of the Brillouin zone has been increased to 2556 *k*-points. This exploration provides valuable insights into the material's behaviour under different conditions.

3. Findings and interpretation

3.1 Structural characteristics

The study involved an improvement of the structural characteristics of perovskite compounds, focusing on their cubic geometry. Fig. 1 in shows a representation of the fully relaxed structure of these compounds. In this cubic structure, the halide ion O is positioned at coordinates (1/2,1/2,*y*) with *y* equal to 0.249, while the constituent atoms Hg and Cr are located at (0,0,0) and (1/2,1/2,1/2), respectively.[11] The analysis revealed that these chemicals possess a cubic *Pm3m* space group, signifying their structural symmetry. To determine the ideal lattice parameters, we employ the PBE-GGA functional and the Birch Murnaghan equation of state against volume (measured

in atomic units) as represented in Fig. 2.[26] This computational approach allows for precise assessments of the lattice parameters, contributing to a deeper understanding of the material's properties and behaviour in the cubic phase.[27] Table 1 displays the structural optimization's computed results. The computed results are discovered to be consistent with past findings, demonstrating the accuracy of our computation. The tolerance factor (τ) to support the cubic structural parameters was also estimated.[23,28,29] The examined chemical is assumed to have a cubic structure if the indicator parameter's value falls within the range of 0.95 and 1.04. Table 1 displays the anticipated value of the, which indicates the cubic structure. Calculating the cohesive energy and formation energy of the investigated $HgCrO_3$ has allowed for the evaluation of its thermodynamic and chemical stabilities,[26,27] as shown in Table 1. Cohesive energy of the solid is the amount of energy required to form separated neutral atoms in their ground electronic state from the solid. A higher degree of stability is associated with higher cohesive energy levels. The cohesive energy per atom can be calculated using the following formula:

$$E_{\text{Cohesive}}^{HgCrO_3} = \frac{1}{3}\left[(E_{Hg} + E_{Cr} + 3E_O) - E_{\text{tot}}^{HgCrO_3}\right] \qquad (1)$$

Here $E_{\text{Cohesive}}^{HgCrO_3}$ refers to the total energy of the unit cell, E_{Hg}, E_{Cr}, $3E_O$ are the total energies of the corresponding elements in their free state of isolated atoms. The computed cohesive energy is 3.05 ev per atom suggesting the chemical stability of the investigated compound. Furthermore formation energy is computed as

$$E_{\text{formation}}^{HgCrO_3} = \frac{1}{3}\left[E_{\text{tot}}^{HgCrO_3} - \left(E_{Hg}^{\text{Bulk}} + E_{Cr}^{\text{Bulk}} + 3E_O^{\text{Bulk}}\right)\right] \qquad (2)$$

$E_{\text{tot}}^{HgCrO_3}$ is the total energy of $HgCrO_3$ per formula unit, and E_{Hg}^{Bulk}, E_{Cr}^{Bulk}, $3E_O^{\text{Bulk}}$ are the total energies of Hg, Cr and O in bulk. Table 1 shows that the compound under investigation has a negative formation energy, indicating that it is thermodynamically stability.[30,31] This stability is essential in understanding the compound's behaviour in various applications, such as in materials science and catalysis. It indicates that $HgCrO_3$ is likely to exist and persist in the examined conditions, making it a valuable material for certain applications.

3.2 Electronic properties

The study of electronic properties is indeed a key component of compounds, crucial for developing materials with specific qualities for various applications. The electronic band structure of a material graphically represents the permissible energy levels for electrons in a solid. This structure is based on how electrons behave in the valence and conduction bands and the gap between them.[32,33] The size of this energy gap determines whether a material is an insulator, semiconductor, or metal. Moreover, a material's electronic properties, such as electrical conductivity, optical characteristics, and magnetic behaviour's, are largely influenced by the behaviours of electrons in these bands and the width of the gap. In this work, $HgCrO_3$, the most stable structure and optimized lattice parameters were likely used to investigate its electrical characteristics.[34,35] This involves
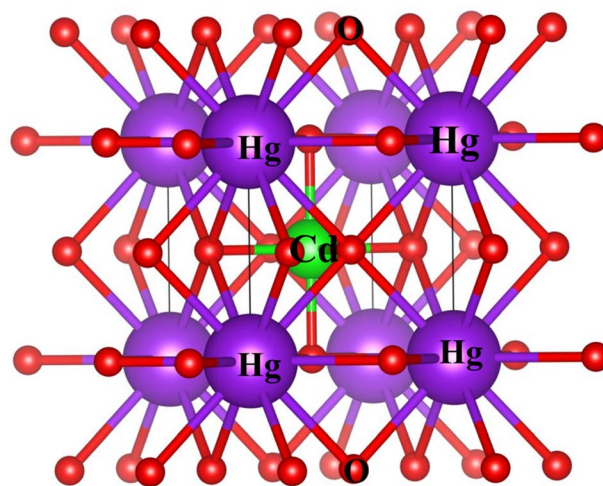

Fig. 1 Computed crystal structure of cubic $HgCrO_3$.

understanding how electrons interact within the material's electronic band structure, which, in turn, affects its overall electronic properties. The electronic band structure of $HgCrO_3$ was investigated using Density Functional Theory (DFT), a powerful computational technique for studying the electronic properties of materials. The electronic properties as computed from the GGA reveals the metallic nature of the $HgCrO_3$ as represented in Fig. 3(a). However again we considered the mBJ method to endeavour the electronic properties in spin up and spin down. It is observed that bandgap exist both in spin up and spin down, only P-type doping occurs when spin up, which may have better electrical conductivity while spin down shows near-intrinsic type as observed in Fig. 3(b).[12,36]

Fig. 4 illustrates the computed total and partial densities of states (TDOS and PDOS) for $HgCrO_3$. These density of states plots provide critical insights into the electronic structure of the material. TDOS gives an overview of all available electronic states at various energy levels. It helps understand the overall electronic behaviour of $HgCrO_3$. PDOS (Partial Density of States)
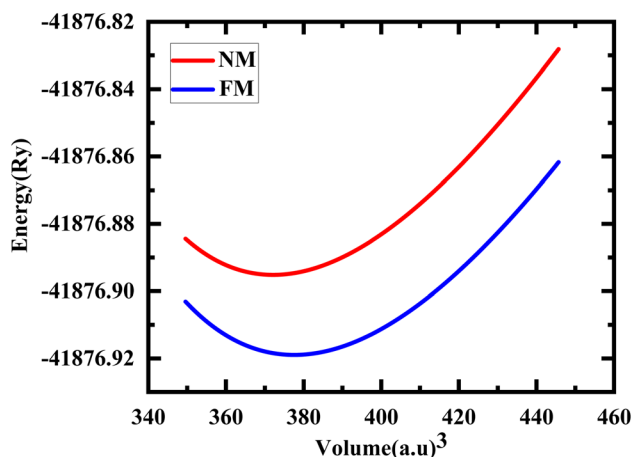

Fig. 2 Total energy with the volume optimization curve of $HgCrO_3$ in its NM, FM phases.

Table 1 The calculated lattice parameters a_0, volume V_0, bulk modulus B_0, the derivative of the bulk B'_0 and equilibrium total energy E_0, cohesive energy (E_c) for HgCrO$_3$ for phases in NM and FM states using GGA-PBE approximation

Compound	Phases	a_0 (Å)	V_0 (a^3)	B'_0	E_{tot} (Ry)	E_f (ev per atom)	E_c (eV per atom)	ΔE (Ry) = $E_{N\,M} - E_{FM}$
HgCrO$_3$	FM	3.82	377.62	190.39	−41876.918940	−2.631	3.05	0.023751
	NM	3.80	372.21	198.99	−41876.895189			
Other[11]		3.76		200.88				

breaks down the electronic states by specifying contributions from individual atoms or orbitals within HgCrO$_3$. This allows for a detailed analysis of how specific elements or orbitals affect the electronic properties.[37–39] The Fermi level, represented by a vertically broken line in the figure, indicates the energy level at which electrons are in their ground state at absolute zero temperature. It's a crucial reference point for understanding the material's conductivity and its classification as a metal, semiconductor, or insulator. Overall, Fig. 4 provides a comprehensive view of the electronic properties of HgCrO$_3$, with TDOS, PDOS, and the Fermi level as key components for analysis. The presence of complete Density of States (DOS) profiles above the Fermi level (E_f) provides indicating the prospect of HgCrO$_3$ revealing metallic conductivity. In metallic materials, the existence of electronic states available for conduction above the Fermi level is a defining characteristic. A major part of the contribution to the Total Density of States (TDOS) in proximity to the Fermi level comes from the Hg (4d/5d) orbitals. Consequently, it can be inferred that the d orbitals associated with Hg atoms play a central role in facilitating the electrical conductivity of both compounds. The attributes characterizing the electronic states pertaining to Hg's 4d/5d bonding orbitals serve as the principal contributors to the chemical and mechanical stability inherent in HgCrO$_3$. These electronic states are instrumental in comprehending the overarching stability exhibited by the material. The TDOS profiles of HgCrO$_3$ framework a prevailing presence of Cr-4d/La-5d orbitals, in conjunction with O 5p and Hg 2p states, within the valence and conduction bands of HgCrO$_3$, specifically in the energy range

spanning from 1.03 eV to 2.25 eV. This elucidates the salient electronic states governing the material's electronic behavior within this energy spectrum. The attractive acknowledges that the Density of States at the Fermi level (E_f, DOSs) wields a pivotal influence on the electrical stability observed in HgCrO$_3$ metallic systems. The position of the Fermi level, (E_F), along with its associated strength, bears significant consequences for the phase stability of intermetallic complexes.[40,41] Notably, complexes characterized by lower E_f values tend to exhibit heightened stability in comparison to those characterized by higher E_f values.

3.3 Magnetic properties

Magnetism, a fundamental property of materials, finds significant applications in various industries, including electronics, energy, and medicine. When studying a material's magnetic characteristics, one crucial parameter to consider is the magnetic moment, which provides insights into the magnetic field's properties and frequency. This investigation investigates the magnetic spin moments of HgCrO$_3$, a complex compound comprising elements such as cadmium (Hg), chromium (Cr), and oxygen (O). To explore its magnetic properties, the total and partial magnetic moments, including polarized spins in the interstitial sites and muffin-tin spheres, were estimated using both the GGA model.[42] The findings, presented in Table 2, reveal that material exhibit metallic characteristics due to their total magnetic moments per cell unit interestingly, the magnetic moments of Hg and O atoms were found to be relatively modest and had a minimal impact on the overall
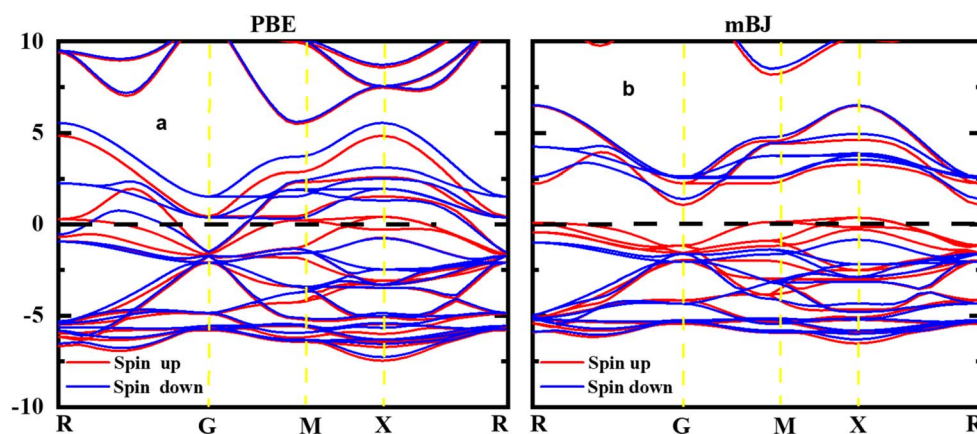

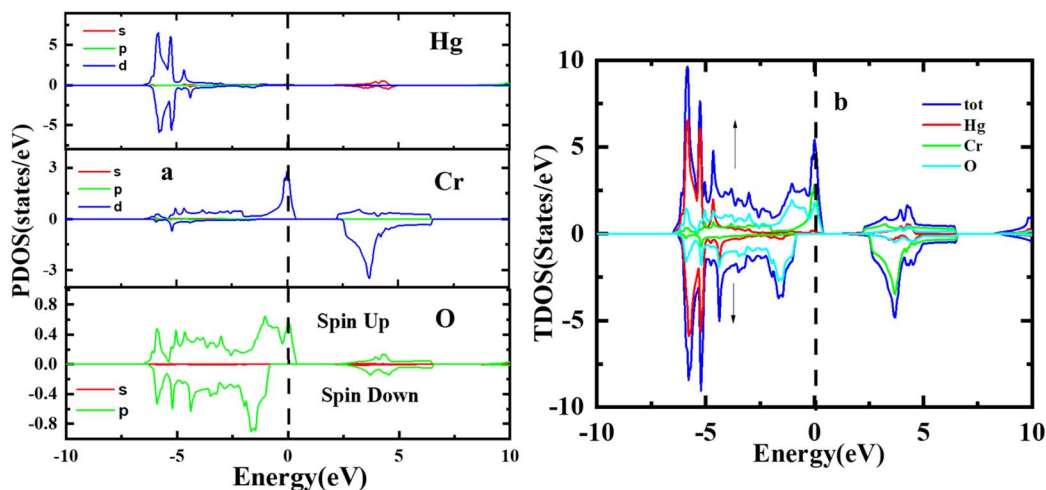**Fig. 3** Spin–polarized band structures of perovskite oxide HgCrO$_3$ spin up and spin down.

Fig. 4 Total and partial density of states of perovskite oxide HgCrO₃.

Table 2 The total and atomic magnetic moments of compounds by different XC (PBE-GGA and mBJ-GGA). M_{tot} (μ_B): total magnetic moment; M_{Ti} (μ_B): Ti magnetic moment; M_{Ti} (μ_B): Ti magnetic moment; M_{Fe} (μ_B): Fe magnetic moment; M_{As} (μ_B): As magnetic moment; M_{Int} (μ_B): the magnetic moment in the interstitial region

XC	PBE	mBJ
$M_{interstitial}$ (μ_B)	0.24	0.27
M_{Hg} (μ_B)	0.08	0.02
M_{Cr} (μ_B)	1.63	2.06
M_O (μ_B)	−0.03	−0.12
M_{tot} (μ_B)	1.88	2.00

magnetic moment. Nevertheless, they play a pivotal role in the emergence of magnetism and influence the major band gap's magnitude in HgCrO₃. This underscores the importance of considering these atoms' magnetic moments when investigating a material's magnetic properties. Furthermore, it was observed that the interstitial region possesses a substantial magnetic moment. This effect can be attributed to a significant charge transfer from Hg and Cr to O, driven by the difference in electronegativity values as represented in Table 2. The high magnetic moment in the interstitial region can have profound implications for the compound's characteristics, including its electrical and optical properties, which are vital for numerous applications.[43] Furthermore, a noteworthy finding is the substantial magnetic moment observed in the interstitial region. This phenomenon can be attributed to a significant charge transfer mechanism, wherein electrons are transferred from Hg and Cr to O. The underlying explanation lies in the contrasting electronegativity values of these elements. Specifically, oxygen (O) is characterized by a higher electronegativity value of 3.5 on the Pauling scale, while both mercury (Hg) and chromium (Cr) exhibit significantly lower electronegativity values, differing by 1.69 units compared to O. This marked difference in electronegativity levels results in a substantial charge transfer from Hg and Cr to O, consequently giving rise to the magnetic moment observed in the interstitial region. The

notable magnetic moment in the interstitial area can wield a profound influence on the compound's overall characteristics, potentially impacting its behavior and properties in various applications.[44] The compound's electrical and optical properties, for instance, which are crucial for a number of applications, might be impacted by the magnetic moment. The magnetic moment in the interstitial region can also affect the stability and symmetry of the compound's structure.

3.4 Thermal characteristics

Using Gibbs2 code,[45] we investigate a comprehensive analysis of the thermodynamic properties of the HgCrO₃ compound. Our investigation has a temperature range spanning from 0 to 1200 K while considering pressure variations from 0 to 196 GPa, employing the quasi-harmonic model. The variation of volume at diverse pressure and temperature is represented in Fig. 5(a) shows it decreases with increase in temperature. One outstanding finding pertains to the bulk modulus (B) of HgCrO₃ at varying conditions. At 0 K, the bulk modulus reaches its peak value of 210 GPa. This observation signifies that as pressure increases at a given temperature, the bulk modulus also increases while maintaining constant pressure results in a decrease in the bulk modulus as seen in Fig. 5(b). Furthermore, it is noteworthy that the bulk modulus remains relatively constant within the temperature range of 0 to 220 K, after which it gradually decreases with rising temperature. Heat capacity at constant volume (C_v) plays a pivotal role in understanding the vibrational properties of compounds.[23] C_v exhibits distinct behavior across temperature ranges as seen in Fig. 5(c). At low temperatures below 300 K, C_v shows a sharp increase with rising temperature, constituting the first phase. Subsequently, in the second phase above 300 K, there is a progressive increase in C_v with temperature. This intricate behavior of heat capacity provides valuable insights into the compound's thermal characteristics as seen Fig. 5(d) illustrates the temperature-dependent changes in the entropy of HgCrO₃. The exponential nature of the entropy curves is evident. At a temperature of 300
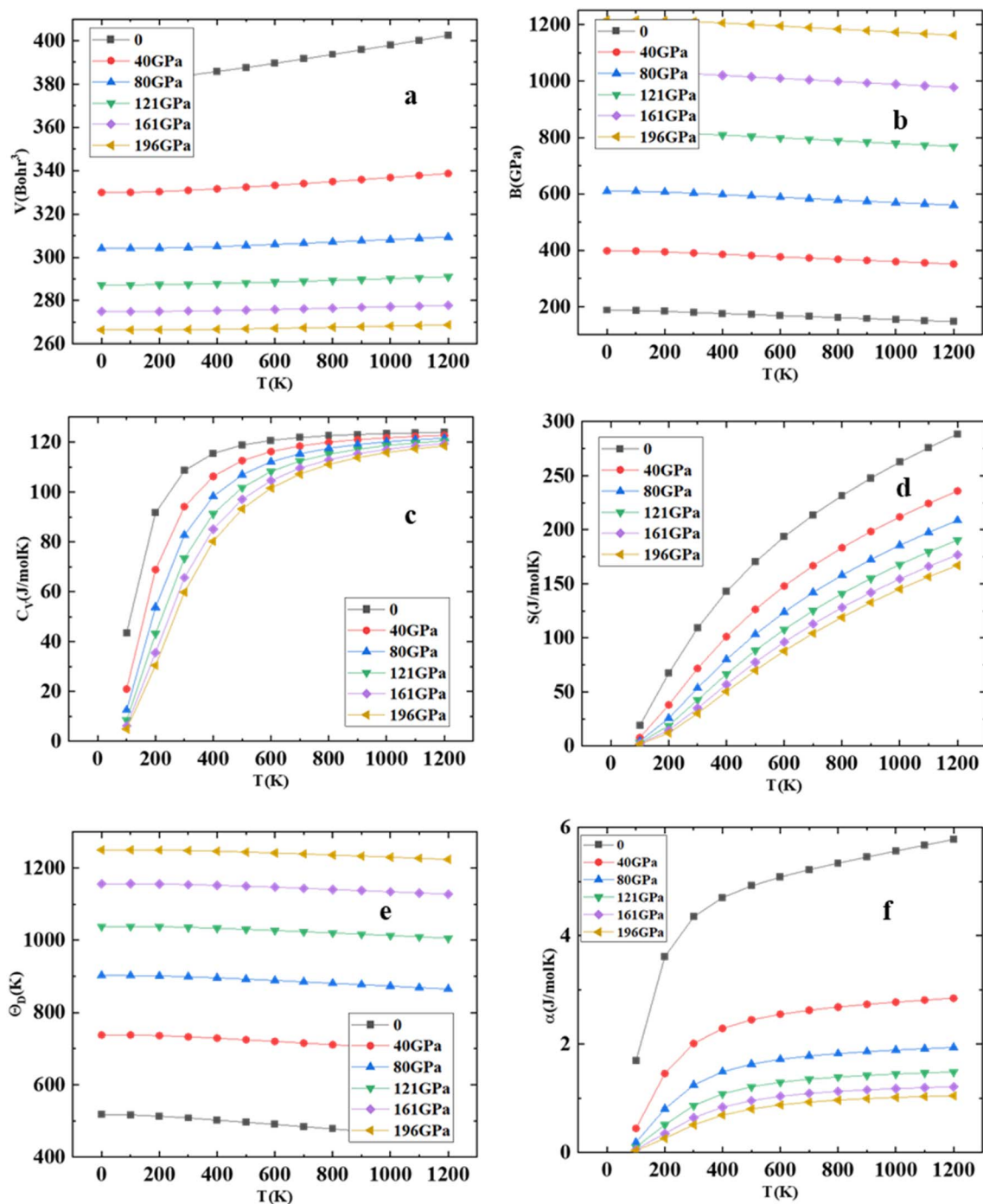
Fig. 5 (a) Volume (V), (b) Bulk modulus (c) heat capacity at constant volume (C_V), (d) entropy (S), (e) Debye temperature (θ_D) and (f) thermal expansion coefficient (α) *versus* the different temperatures for HgCrO$_3$.

K and under normal pressure conditions, the entropy of the tested HgCrO$_3$ compound is approximately 121.66 J mol^{-1} K^{-1}. This data is valuable for evaluating the structural stability of compounds.[23,38] Additionally, the thermal expansion coefficient, denoted as $\alpha(T)$, serves as a key indicator of structural stability. Additionally, we computed the Debye temperature (θ_D) for HgCrO$_3$, as presented in Fig. 5(e). Notably, the calculated (θ_D) values for HgCrO$_3$ are 575 at 0 K and 40 GPa pressure.

Linear declines in (θ_D) occur under constant pressure and temperature conditions. It is noteworthy that the effect of pressure serves to elevate the Debye temperature (θ_D)) with increasing pressure and temperature.[46,47] This comprehensive analysis of thermodynamic characteristics contributes valuable insights that can inform experimental efforts in understanding the behaviour of HgCrO$_3$ under varying temperature and pressure conditions. As depicted in Fig. 5(f), exhibit a substantial
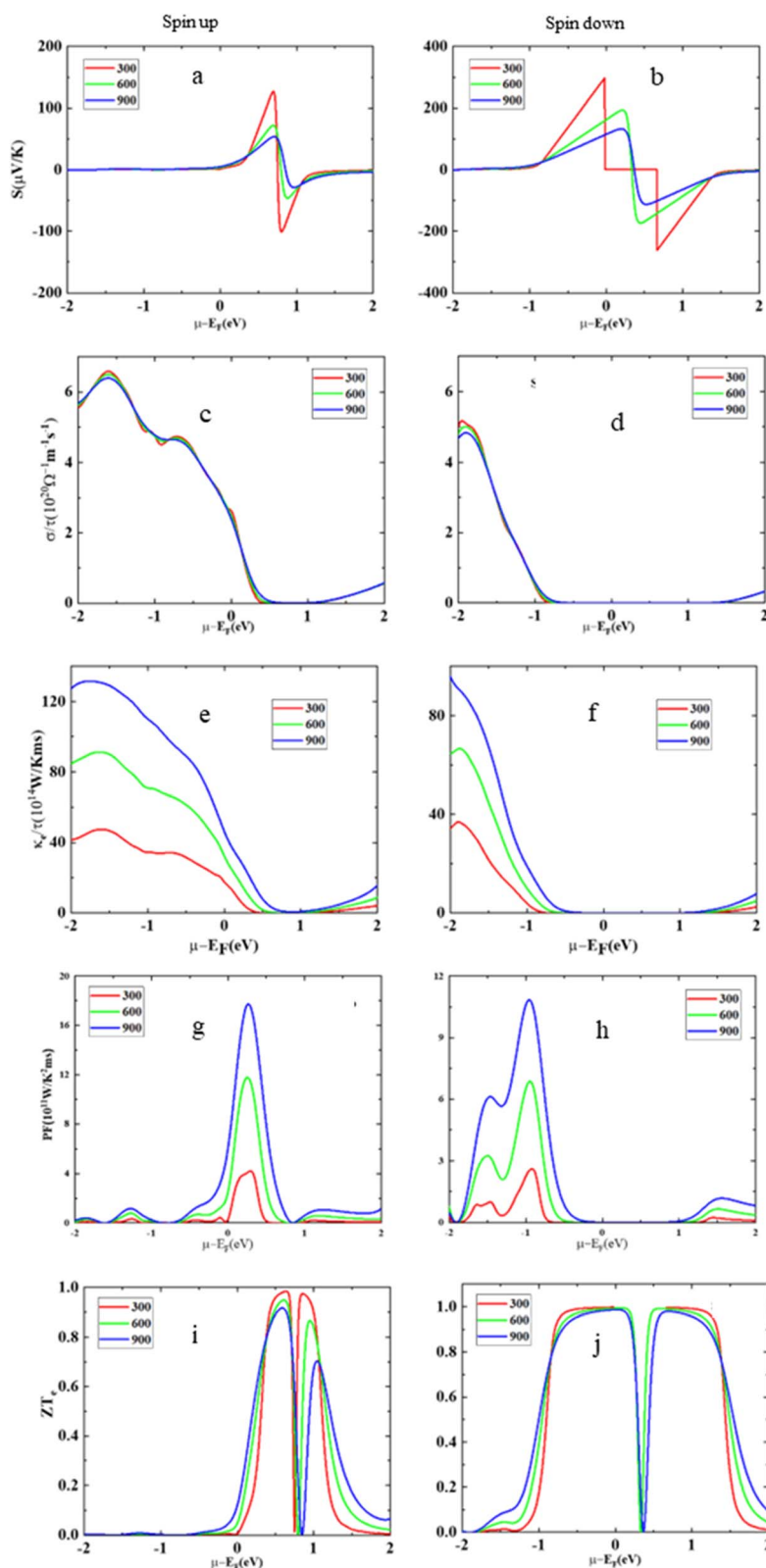
Fig. 6 The Seebeck coefficient (S) (a) spin-up, (b) spin-down, electrical conductivity (σ/τ), (c) spin-up, (d) spin-down, electronic thermal conductivity (κ_e/τ) (e) spin-up, (f) spin-down, power factor ($S^2\sigma$) (g) spin-up, and (h) spin-down, figure of merit (ZT) (i) spin-up, and (j) spin-down versus the chemical potential (μ) at different temperatures for HgCrO$_3$.

increase in $\alpha(T)$ up to 200 K due to the influence of the harmonic component of the Debye model approximation. However, beyond this temperature threshold, the thermal expansion coefficient consistently decreases, highlighting the HgCrO$_3$ crystal's remarkable volume invariance.

3.5 Transport characteristics

This section of the study focuses on thermoelectric materials, which have significant attention worldwide due to their unique ability to convert thermal energy into usable electricity and *vice versa*. These materials are highly sought after, particularly within the thermoelectric field, because of their dielectric properties and their capability to harness and produce energy. The primary goal of this section is to conduct a comprehensive investigation into various transport coefficients associated with HgCrO$_3$. These coefficients are assessed for both the up-spin and down-spin states of the material. The key parameters under scrutiny encompass electrical conductivity (σ/τ), which provides insights into the material's efficiency in conducting electricity[35] Seebeck coefficient (S), which quantifies a material's ability to generate voltage when exposed to a temperature gradient, thereby facilitating the conversion of heat into electrical energy. Additionally, the figure of merit (ZT), a critical metric in the realm of thermoelectric materials, is evaluated to gauge the material's overall thermoelectric performance. It combines information from electrical conductivity, the Seebeck coefficient, and thermal conductivity to assess the material's efficiency in converting heat into electricity. Fig. 6(a and b) is a graphical representation of the variations in the Seebeck coefficient (S) for a material called HgCrO$_3$ at different temperatures. The Seebeck coefficient is a measure of a material's ability to generate an electric voltage when subjected to a temperature gradient, which is crucial in thermoelectric applications. The key findings *i.e.* up-spin state, when HgCrO$_3$ is in the up-spin state (a particular electronic configuration or condition), the Seebeck coefficient remains positive across the entire temperature range. This means that the material consistently generates a positive electric voltage when exposed to temperature differences in this state. The positive value indicates that HgCrO$_3$ has a thermoelectric behaviour that is favourable for generating electricity from heat. Spin-down state, In the spin-down state of HgCrO$_3$ (another electronic configuration or condition), the Seebeck coefficient increases linearly with temperature throughout the entire temperature spectrum. This suggests that, in this state, as the temperature rises, the material's ability to generate electric voltage also increases in a predictable, linear fashion. This behaviour is essential for understanding how HgCrO$_3$ performs in different electronic states and temperature conditions, which is critical information for thermoelectric applications. Overall, this figure provides valuable insights into the thermoelectric properties of HgCrO$_3$ under different conditions and temperatures, which can be helpful for designing thermoelectric devices and applications. In Fig. 6(c and d), the data reveals the temperature-dependent behaviour of electrical conductivity (σ/τ) in HgCrO$_3$. Notably, it is important to highlight that the computed electrical

conductivity values for the spin-up electron state differ from those obtained for the spin-down electron state, as documented in ref. 45. Specifically, for the spin-up state, the electrical conductivity (σ/τ) exhibits an increase between temperatures of 300 Kelvin to 900 Kelvin. In contrast, for the spin-down state, there is a decrease in electrical conductivity within the temperature range of 200 Kelvin to 800 Kelvin. The thermal conductivity as represented in Fig. 6(e and f) shows variation with different temperatures. The less thermal conductivity advocates its optimum thermoelectric performance. The power factor reflects the thermoelectric applicability of these compounds as represented in Fig. 6(g and h). Moreover, Fig. 6(i and j) provides an overview of the changes in the figure of merit (ZT) across a temperature range spanning from 0 Kelvin to 800 Kelvin, which enables an evaluation of the thermoelectric efficiency of the compound, the discussion highlights that at a temperature of 300 Kelvin, the figure of merit (ZT) values for HgCrO$_3$ are nearly negligible, indicating limited thermoelectric efficiency at this temperature. However, as the temperature rises, there is a noticeable improvement in the ZT values, suggesting that HgCrO$_3$ becomes more suitable for thermoelectric applications at higher temperatures.[48] This observation is significant because it implies that HgCrO$_3$ has the potential to be practically utilized in technologies related to energy conversion and utilization, particularly at elevated temperatures where its thermoelectric performance becomes more favourable.

4. Conclusions

Comprehensive study, we conducted an in-depth examination of various aspects of HgCrO$_3$ perovskite, including its structural, elastic, vibrational, and thermodynamic characteristics. To achieve this, we utilized advanced computational methods, specifically the FP-LAPW (Full-Potential Linearized Augmented Plane Wave) and quasi-harmonic Debye models. We optimized the lattice parameters of HgCrO$_3$ using the generalized gradient approximation of the Perdew–Burke and Ernzerhof exchange-correlation functional (GGA-PBE). The results from these optimizations align well with previous research, confirming the accuracy of our calculations. Our findings indicate that both materials under investigation exhibit metallic properties, as evidenced by their electronic energy band structures and overall density of states. Additionally, we identified that the conductivity of both materials is primarily governed by Hg-4d electronic orbitals, further characterizing their electronic behavior. Through the quasi-harmonic Debye model, we delved into several key thermodynamic properties, including the relative Debye temperature, thermal expansion parameter, relative volume, and heat capacity at various temperatures and pressures. Notably, we determined that the heat capacity at constant volume is approximately 52 J mol^{-1} K^{-1}. Furthermore, our analysis revealed that the HgCrO$_3$ compound demonstrates excellent volume invariance when exposed to high temperatures, as indicated by the coefficient of thermal expansion. It's important to note that this research contributes to a broader theoretical project that encompasses a comprehensive

understanding of this molecule, enhancing our knowledge of its characteristics and behaviour.

Conflicts of interest

There are no conflicts to declare.

Acknowledgements

References

1 H. Liu and X. Yang, A Brief Review on Perovskite Multiferroics, *Ferroelectrics*, 2017, **507**, 69–85.

2 S. Bağcı, B. G. Yalçın, H. M. Tütüncü and G. P. Srivastava, Ground State, Phonon Spectrum, and Superconducting Properties of the Cubic Inverse Perovskite Sc₃AlN, *Phys. Rev. B: Condens. Matter Mater. Phys.*, 2010, **81**, 54523.

3 D. Behera and S. K. Mukherjee, Theoretical Investigation of the Lead-Free K2InBiX6 (X= Cl, Br) Double Perovskite Compounds Using First Principle Calculation, *JETP Lett.*, 2022, **116**, 533–534.

4 S. Al-Qaisi, H. Rached, T. A. Alrebdi, S. Bouzgarrou, D. Behera, S. K. Mukherjee, M. Khuili, M. Adam, A. S. Verma and M. Ezzeldien, Study of Mechanical, Optical, and Thermoelectric Characteristics of Ba2XMoO6 (X= Zn, Cd) Double Perovskite for Energy Harvesting, *J. Comput. Chem.*, 2023, **44**, 2442–2452.

5 C. Li, K. C. K. Soh and P. Wu, Formability of ABO3 Perovskites, *J. Alloys Compd.*, 2004, **372**, 40–48.

6 R. S. Roth, Classification of Perovskite and Other ABO3-Type Compounds, *J. Res. Natl. Bur. Stand.*, 1957, **58**, 75.

7 B. Sun, G. Zhou, L. Sun, H. B. Zhao, Y. Chen, F. Yang, Y. Zhao and Q. L. Song, ABO3 Multiferroic Perovskite for Memristive Memory and Neuromorphic Computing, *Nanoscale Horiz.*, 2021, **6**, 939–970.

8 A. A. Emery and C. Wolverton, High-Throughput DFT Calculations of Formation Energy, Stability and Oxygen Vacancy Formation Energy of ABO3 Perovskites, *Sci. Data*, 2017, **4**, 1–10.

9 N. Xu, H. Zhao, X. Zhou, W. Wei, X. Lu, W. Ding and F. Li, Dependence of Critical Radius of the Cubic Perovskite ABO3 Oxides on the Radius of A-and B-Site Cations, *Int. J. Hydrogen Energy*, 2010, **35**, 7295–7301.

10 S. Behara, T. Poonawala and T. Thomas, Crystal Structure Classification in ABO3 Perovskites via Machine Learning, *Comput. Mater. Sci.*, 2021, **188**, 110191.

11 S. Satapathy, M. Batouche, T. Seddik, M. M. Salah and K. K. Maurya, First Principle Study on Structural, Thermoelectric, and Magnetic Properties of Cubic CdCrO3 Perovskites: A Comprehensive Analysis, *Crystals*, 2023, **13**, 1185.

12 Z. Ali, I. Ahmad, B. Khan and I. Khan, Robust Half-Metallicity and Magnetic Properties of Cubic Perovskite CaFeO3, *Chin. Phys. Lett.*, 2013, **30**, 47504.

13 Z. Aboub, T. Seddik, B. Daoudi, A. Boukraa, D. Behera, M. Batouche and S. K. Mukherjee, Impact of La, Ni-Doping on Structural and Electronic Properties of SrTiO3 for Photocatalytic Water Splitting, *Inorg. Chem. Commun.*, 2023, 110871.

14 M. Yaseen, H. Ambreen, J. Iqbal, A. Shahzad, R. Zahid, N. A. Kattan, S. M. Ramay and A. Mahmood, Electronic, Optical and Magnetic Properties of PrXO3 (X= V, Cr): First-Principle Calculations, *Philos. Mag.*, 2020, **100**, 3125–3140.

15 M. Rashid, M. A. Iqbal and N. A. Noor, DFT-MBJ Study of Electronic and Magnetic Properties of Cubic CeCrO3 Compound: An Ab-Initio Investigation, *Sci. J. Rev.*, 2017, **1**, 27–36.

16 L. H. Yin, T. F. Shi, R. R. Zhang, C. B. Park, K. H. Kim, J. Yang, P. Tong, W. H. Song, J. M. Dai and X. B. Zhu, Electric Dipoles via C r 3+(d 3) Ion off-Center Displacement in Perovskite DyCr O 3, *Phys. Rev. B: Condens. Matter Mater. Phys.*, 2018, **98**, 54301.

17 L. H. Yin, J. Yang, P. Tong, X. Luo, C. B. Park, K. W. Shin, W. H. Song, J. M. Dai, K. H. Kim and X. B. Zhu, Role of Rare Earth Ions in the Magnetic, Magnetocaloric and Magnetoelectric Properties of RCrO 3 (R= Dy, Nd, Tb, Er) Crystals, *J. Mater. Chem. C*, 2016, **4**, 11198–11204.

18 P. Hohenberg and W. Kohn, Density Functional Theory (DFT), *Phys. Rev.*, 1964, **136**, B864.

19 D. Behera, B. Akila, R. Amraoui, S. Kadri, S. K. Mukherjee, M. M. Salah and A. Saeed, Excellent Thermoelectric Performance in KBaTh (Th= Sb, Bi) Based Half-Heusler Compounds and Design of Actuator for Efficient and Sustainable Energy Harvesting Applications, *Crystals*, 2023, **13**, 1551.

20 P. Blaha, K. Schwarz, P. Sorantin and S. B. Trickey, Full-Potential, Linearized Augmented Plane Wave Programs for Crystalline Systems, *Comput. Phys. Commun.*, 1990, **59**, 399–415.

21 P. Blaha, K. Schwarz, G. K. H. Madsen, D. Kvasnicka and J. Luitz, *Wien2k: An Augmented Plane Wave Plus Local Orbitals Program for Calculating Crystal Properties*, 2001.

22 D. Behera and S. K. Mukherjee, First-Principles Calculations to Investigate Structural, Optoelectronics and Thermoelectric Properties of Lead Free Cs2GeSnX6 (X= Cl, Br), *Mater. Sci. Eng. B*, 2023, **292**, 116421.

23 M. Manzoor, D. Behera, R. Sharma, M. W. Iqbal and S. K. Mukherjee, First Principles Insights on the Structural, Mechanical, Dynamical, Thermoelectric and Thermodynamics Properties of Novel Topological (ScSb) Semi-Metal, *Mater. Sci. Eng. B*, 2023, **291**, 116372.

24 G. K. H. Madsen and D. J. Singh, BoltzTraP. A Code for Calculating Band-Structure Dependent Quantities, *Comput. Phys. Commun.*, 2006, **175**, 67–71.

25 D. Behera, B. Akila, S. K. Mukherjee, T. A. Geleta, A. Shaker and M. M. Salah, Studies on Optoelectronic and Transport

Properties of XSnBr3 (X= Rb/Cs): A DFT Insight, *Crystals*, 2023, **13**, 1437.

26 T. Katsura and Y. Tange, A Simple Derivation of the Birch–Murnaghan Equations of State (EOSs) and Comparison with EOSs Derived from Other Definitions of Finite Strain, *Minerals*, 2019, **9**, 745.

27 D. Behera, J. A. Abraham, R. Sharma, S. K. Mukerjee and E. Jain, First Principles Study of New D0 Half-Metallic Ferromagnetism in CsBaC Ternary Half-Heusler Alloy, *J. Supercond. Novel Magn.*, 2022, **35**, 3431–3437.

28 A. E. Fedorovskiy, N. A. Drigo and M. K. Nazeeruddin, The Role of Goldschmidt's Tolerance Factor in the Formation of A2BX6 Double Halide Perovskites and Its Optimal Range, *Small Methods*, 2020, **4**, 1900426.

29 D. Behera, M. Manzoor, R. Sharma, M. W. Iqbal and S. K. Mukherjee, First Principles Insight on Structural, Opto-Electronic and Transport Properties of Novel Zintl-Phase AMg2Bi2 (A= Sr, Ba), *J. Solid State Chem.*, 2023, **320**, 123860.

30 S. Lakra and S. Kumar Mukherjee, Study of Structural, Electronic, Optical and Thermodynamic Properties of SnSiO3 Compound: A DFT Study, *Mater. Today: Proc.*, 2023, DOI: 10.1016/j.matpr.2023.01.231.

31 T. Seddik, D. Behera, M. Batouche, W. Ouerghui, H. B. Abdallah, R. K. Sarkar, M. M. Salah, A. Shaker and S. K. Mukherjee, Electronic Properties, Linear and Nonlinear Performance of KAg Ch (Ch= S, Se) Compounds: A First-Principles Study, *Crystals*, 2023, **13**, 726.

32 Y. O. Ciftci and S. D. Mahanti, Electronic Structure and Thermoelectric Properties of Half-Heusler Compounds with Eight Electron Valence Count—KScX (X= C and Ge), *J. Appl. Phys.*, 2016, **119**, 145703.

33 T. Ahmed, A. Chen, D. A. Yarotski, S. A. Trugman, Q. Jia and J.-X. Zhu, Magnetic, electronic, and optical properties of double perovskite Bi2FeMnO6, *APL Mater.*, 2017, **5**, 035601.

34 D. Vasileska, H. R. Khan, S. S. Ahmed, G. Kannan and C. Ringhofer, Quantum and Coulomb Effects in Nano Devices, in *Nano-Electronic Devices*, Springer, 2011, pp. 97–181.

35 D. Behera and S. K. Mukherjee, Structural, Elastic, Electronic and Thermoelectric Properties of K2GeBr6: A First Principle Approach, *Mater. Today: Proc.*, 2023, DOI: 10.1016/j.matpr.2023.01.338.

36 D. Behera, A. Dixit, K. Kumari, A. Srivastava, R. Sharma, S. K. Mukherjee, R. Khenata, A. Boumaza and S. Bin-Omran, Structural, Elastic, Mechanical, and Thermodynamic Characteristic of NaReO3 and KReO3 Perovskite Oxides from First Principles Study, *Eur. Phys. J. Plus*, 2022, **137**, 1345.

37 A. Candan and M. Kurban, Electronic Structure, Elastic and Phonon Properties of Perovskite-Type Hydrides MgXH3 (X= Fe, Co) for Hydrogen Storage, *Solid State Commun.*, 2018, **281**, 38–43.

38 D. Behera, A. Dixit, B. Nahak, A. Srivastava, R. Sharma, R. Khenata, S. Bin-Omran, S. A. M. Abdelmohsen, A. M. M. Abdelbacki and S. K. Mukherjee, Theoretical Insight on the Electronic Band Structure, Mechanical, Vibrational and Thermodynamic Characteristic of Antiperovskites RE3InN (RE= Y and La), *Mater. Today Commun.*, 2023, **35**, 105618.

39 A. Dixit, A. Saxena, D. Behera, J. A. Abraham, R. Sharma and S. K. Mukherjee, First Principles Study on Structural, Mechanical, and Thermoelectric Properties of Half-Heusler Alloy (KLiTe), *Mater. Today: Proc.*, 2023, DOI: 10.1016/j.matpr.2023.02.093.

40 A. Saxena, A. Dixit, D. Behera, J. A. Abraham, R. Sharma and S. K. Mukherjee, Insight on Structural, Electronic and Thermoelectric Properties of Perovskite AgBaCl3 by an Ab-Initio for Solar Cell and Renewable Energy, *Mater. Today: Proc.*, 2023, DOI: 10.1016/j.matpr.2023.02.288.

41 D. Behera, A. Azzouz-Rached, A. Bouhenna, M. M. Salah, A. Shaker and S. K. Mukherjee, First-Principles Studies on the Physical Properties of the Half Heusler RbNbCd and RbNbZn Compounds: A Promising Material for Thermoelectric Applications, *Crystals*, 2023, **13**, 618.

42 R. Benabboun, D. Mesri, A. Tadjer, A. Lakdja and O. Benhelal, Half-Metallicity Ferromagnetism in Half-Heusler XCaZ (X= Li, Na; Z= B, C) Compounds: An Ab Initio Calculation, *J. Supercond. Novel Magn.*, 2015, **28**, 2881–2890.

43 S. A. Dar, V. Srivastava, U. K. Sakalle and V. Parey, Electronic Structure, Magnetic, Mechanical and Thermo-Physical Behavior of Double Perovskite Ba2MgOsO6, *Eur. Phys. J. Plus*, 2018, **133**, 1–12.

44 G. Li, H. Ahmoum, S. Liu, S. Liu, M. S. Su'ait, M. Boughrara, M. Kerouad and Q. Wang, Theoretical Insight into Magnetic and Thermoelectric Properties of Au Doped ZnO Compounds Using Density Functional Theory, *Phys. B*, 2019, **562**, 67–74.

45 M. A. Blanco, E. Francisco and V. G. I. B. B. S. Luana, Isothermal-Isobaric Thermodynamics of Solids from Energy Curves Using a Quasi-Harmonic Debye Model, *Comput. Phys. Commun.*, 2004, **158**, 57–72.

46 K. Bidai, M. Ameri, S. Amel, I. Ameri, Y. Al-Douri, D. Varshney and C. H. Voon, First-Principles Calculations of Pressure and Temperature Dependence of Thermodynamic Properties of Anti-Perovskite BiNBa3 Compound, *Chin. J. Phys.*, 2017, **55**, 2144–2155.

47 S. A. Dar, R. Sharma, V. Srivastava and U. K. Sakalle, Investigation on the Electronic Structure, Optical, Elastic, Mechanical, Thermodynamic and Thermoelectric Properties of Wide Band Gap Semiconductor Double Perovskite Ba 2 InTaO 6, *RSC Adv.*, 2019, **9**, 9522–9532.

48 D. Behera, M. Manzoor and S. K. Mukherjee, Incorporation of Te in Enhancing Thermoelectric Response of AeAg2SeTe (Ae= Sr, Ba) Compounds: A DFT Insight, *Comput. Condens. Matter*, 2022, **33**, e00757.